Anomalous pressure dependence of thermal conductivities of large mass ratio compounds

L. Lindsay, D. A. Broido, Jesús Carrete, Natalio Mingo, and T. L. Reinecke

Phys. Rev. B **91**, 121202 — Published 27 March 2015

DOI: 10.1103/PhysRevB.91.121202

Anomalous pressure dependence of thermal conductivities of large mass ratio compounds

L. Lindsay[1], D. A. Broido[2], Jesús Carrete[3], Natalio Mingo[3], and T. L. Reinecke[4]

[1]Materials Science and Technology Division, Oak Ridge National Laboratory, Oak Ridge, Tennessee 37831, USA

[2]Department of Physics, Boston College, Chestnut Hill, Massachusetts 02467, USA

[3]LITEN, CEA-Grenoble, 17 rue des Martyrs, 38054 Grenoble Cedex 9, France

[4]Naval Research Laboratory, Washington, DC 20375, USA

Abstract

The lattice thermal conductivities (κ) of binary compound materials are examined as a function of hydrostatic pressure, *P*, using a first-principles approach. Compounds with relatively small mass ratios, such as MgO, show an increase in κ with *P*, consistent with measurements. Conversely, compounds with large mass ratios that create significant frequency gaps between acoustic and optic phonons (*e.g.*, BSb, BAs, BeTe, BeSe) exhibit decreasing κ with increasing *P*, a behavior that cannot be understood using simple theories of κ. This anomalous *P* dependence of κ arises from the fundamentally different nature of the intrinsic scattering processes for heat-carrying acoustic phonons in large mass ratio compounds compared to those with small mass ratios. This work demonstrates the power of first principles methods for thermal properties and advances a new paradigm for understanding thermal transport in non-metals.

PACS: 66.70.-f, 63.20.kg, 71.15.-m

Introduction— Pressure dependence gives important insight into the understanding of a range of key materials properties. In 1924, Bridgman published the first measurements of thermal conductivities, κ, of several non-metallic solids as a function of compressive hydrostatic pressure, P [1]. κ for these compounds increased with P from that at ambient pressure (*i.e.*, P=0). Since then, measurements of the pressure dependence of κ have been made in numerous non-metals including alkali halides [2-4], CuCl [5], ice [6, 7], and those residing in the earth's interior, such as MgO [8, 9]. In all systems not approaching a pressure-induced phase transition (PIPT) [10], κ was found to increase with P, suggesting that this is a universal feature.

Explanations of the pressure dependence of κ in non-metallic crystalline materials have typically relied on the theory of Liebfried and Schlömann (LS) [11], which predicts that κ must increase with P [12], *i.e.*, $d\kappa/dP>0$. However, LS gives an empirical description of κ that relies on a number of approximations, which leads one to ask: Is $d\kappa/dP>0$ really a universal property of materials, or are there materials for which $d\kappa/dP<0$? What are the underlying physical properties that govern $d\kappa/dP$?

To address these questions, we have implemented first principles calculations of pressure dependent phonon thermal transport in a large range of materials. We show that for a class of materials κ decreases with P, *i.e.*, $d\kappa/dP<0$, a behavior not previously observed or thought possible for materials far from a PIPT. In binary compounds, this anomalous behavior occurs when the mass ratio of the atoms is large enough to eliminate most of the intrinsic scattering of the heat-carrying acoustic phonons by optic phonons.

First principles thermal transport—Intrinsic thermal resistance in non-metals arises from the anharmonicity of the interatomic potential, which causes interactions between phonons [13]. For the cubic systems examined here, the thermal conductivity is a scalar:

$$\kappa = \kappa_{\alpha\alpha} = \frac{1}{3}\sum_{\lambda} C_\lambda v_\lambda^2 \tau_\lambda \qquad (1)$$

where the sum is over phonon modes $\lambda = (\mathbf{q}, j)$ with $\mathbf{q}$ the phonon wave vector and j the phonon polarization, ω_λ is the phonon frequency, $C_\lambda = \hbar\omega_\lambda(\partial n_\lambda^0 / \partial T)/V$ is the mode specific heat at constant volume, $n_\lambda^0 = 1/(\exp(\hbar\omega_\lambda / k_B T) - 1)$ is the Bose distribution, V is the crystal volume, v_λ is the group velocity, and τ_λ is the phonon transport lifetime obtained from the non-equilibrium phonon distribution, $n_\lambda = n_\lambda^0 + n_\lambda^1$ [14, 15].

The first principles approach for determining κ has been described previously [16-29], including examination of κ as a function of P [27-29]. This approach has no adjustable parameters and has demonstrated very good agreement with measured κ for a variety of systems, which has validated its predictive capability. The present approach uses a full, iterative solution of the Peierls-Boltzmann equation for n_λ^1. The only inputs are harmonic and anharmonic interatomic force constants (IFCs). The harmonic IFCs were calculated within density functional perturbation theory [30] using the Quantum Espresso package [31, 32]. Calculations used the local density approximation and norm-conserving pseudopotentials for the core electrons. Typically, an 80-100 Ryd plane-wave energy cutoff was used with 6x6x6 k-point meshes for the electronic structure and phonon integrations. Anharmonic IFCs were calculated within density functional theory [33, 34] using 80-100 Ryd plane-wave energy cutoffs and gamma point calculations in 216 atom supercells with interactions from 3rd or 5th nearest neighbors of the unit cell atoms. Further details are in Ref. 21. The harmonic IFCs give the phonon frequencies, velocities and specific heat. Anharmonic IFCs are required for the three-phonon scattering rates. We take κ to be limited by only intrinsic three-phonon scattering [35]. The ground state is determined by adjusting the lattice constant, a, to minimize the total energy. For each system,

we decrease a from this value to get a hydrostatic pressure [31], at which we calculate the harmonic and anharmonic IFCs.

Results—We have calculated the pressure dependence of κ for a large number of elemental, III-V and II-VI cubic compounds. We have chosen cubic materials in part because the isotropy of κ gives simpler and more intuitive changes in κ with P. Here, we provide illustrative results for: MgO, GaAs, SiC, BN, BP, BSb, BAs, BeTe, and BeSe, a set of compounds with widely varying mass ratios (see Table I). The last four have much larger mass ratios of constituent atoms than do the first five. This gives qualitatively different pressure dependences of κ. We note that for the materials considered here pressures are far less than those at which measured or calculated phase transitions occur, *e.g.*, BAs (125 GPa) [38], BeSe (56 GPa) [39], BeTe (35 GPa) [39], and BSb P=56 GPa [40]. For several compounds we examined—CuCl, Si, Ge, AlSb, InAs and InSb—calculated TA frequencies soften significantly with small applied P, indicating an approach to a PIPT. We did not include these materials here since the focus of the present paper is identifying and explaining novel thermal transport behavior for which conventional theory fails both qualitatively and quantitatively in predicting κ(P).

Figure 1 shows the phonon dispersions for cubic MgO, an important constituent of the earth's lower mantle whose P dependent κ has attracted wide attention [8, 9, 27]. The calculated phonon frequencies for both P=0 and P>0 agree well with measurements reflecting the accuracy of our harmonic IFCs. Note that increasing P increases phonon frequencies.

The left panel in Fig. 2 gives the calculated and measured [9] κ for MgO as a function of P at T=300K. Inclusion of phonon scattering by isotopes, impurities and sample boundaries [44, 45] gives reasonable agreement with the measured κ and confirms $d\kappa/dP>0$. Calculated κ/κ_0 versus P for BSb, BAs, BeTe and BeSe are shown in the right panel. Values for κ_0, the isotopically

pure κ at P=0, are given in Table I. Although the changes in the phonon dispersions of these large mass ratio compounds with P are similar to those in MgO (see Fig. S1 in Ref. 46), κ *decreases* with P, opposite to the expected behavior. Table I illustrates this distinction between the small and large mass ratio compounds for a number of materials. Note that, in contrast to the *ab initio* results, the LS theory (discussed below) gives $d\kappa/dP>0$ for all materials. We explain the different behaviors in terms of the fundamentally different scattering processes that govern κ in these systems.

Eq. 1 shows that $\kappa(P)$ can be expressed in terms of two features: changes in specific heat and phonon velocities ($C_\lambda v_\lambda^2$), and changes in phonon lifetimes (τ_λ). For the large range of materials examined here, the change in κ with P is governed primarily by changes in phonon lifetimes. *Thus, in order for κ to decrease with increasing P, phonon lifetimes must decrease.*

To understand how τ_λ changes with P, we group three-phonon scattering processes according to the number of participating acoustic (*a*) and optic (*o*) phonons. While heat is carried primarily by acoustic phonons, their scattering by optic phonons contributes significantly to thermal resistance. Typically, two intrinsic three-phonon scattering processes dominate: $a+a \leftrightarrow a$ (*aaa*) and $a+a \leftrightarrow o$ (*aao*) (see Fig. S2 in Ref. 46). For materials with large LO-TO splitting, *aoo* processes can also give non-negligible contributions at low frequency. However, for the materials considered here, the behavior of κ is still dominated by *aaa* and *aao* processes. Changes in τ_λ can be understood from the *aaa* and *aao* contributions to the phonon-phonon scattering rates and their P dependence. A key factor is the size of the frequency gap between acoustic and optic phonon branches (*a*-*o* gap). For small *a*-*o* gap materials, such as MgO, both *aaa* and *aao* processes play significant roles in limiting κ. With increasing P, *aao* scattering rates typically decrease (see Fig. S3 in Ref. 46) because the upward shift of the optic modes

gives decreased optic phonon populations and decreased phase space of *aao* processes, defined below. This reduction dominates the change in κ giving $d\kappa/dP>0$ (see Table I) around room temperature, in qualitative agreement with measured data [2-4, 6-10]. It is interesting that the value $(d\kappa/dP)/\kappa_0=0.009$ GPa^{-1} given in Table I for BN (also obtained independently from the ShengBTE code [47]) is significantly larger than that given in Ref. 29, which gives $(d\kappa/dP)/\kappa_0=0.003$ GPa^{-1} for $P<114$ GPa. Further, our calculations give a roughly linear dependence of κ with P up to $P=300$ GPa, unlike that in Ref. 29. The anharmonic IFCs calculated in the present work simultaneously satisfy point-group and derivative permutation symmetries and translational invariance conditions. This was not the case for anharmonic IFCs used in Ref. 29 and resulted in low-frequency scattering rates that were too large, which then gave suppressed and bimodal behavior of κ (P) for BN (see Fig. 1b of Ref. 29) compared to the larger κ(P) values and linear trend for BN obtained by us.

In contrast to κ(P) for the small mass ratio materials, the κ for BSb, BAs, BeTe and BeSe decrease with P. To understand this behavior, note that the size of the *a-o* gap is controlled in part by the mass ratio, m_{heavy}/m_{light}, of the atoms. As m_{heavy}/m_{light} increases from one (the smallest possible value) the *a-o* gap increases. For sufficiently large m_{heavy}/m_{light}, the *a-o* gap becomes so large that *aao* processes are no longer possible because phonon energy and momentum cannot be conserved. This *aao* freeze-out condition occurs roughly when the *a-o* gap exceeds the maximum acoustic phonon frequency, which is satisfied for the large mass ratio compounds in Fig. 2 (see Table I). In such cases, τ_λ and κ depend on *aaa* scattering. Acoustic phonon branches are typically bunched together in large mass ratio compounds. In these, TA and LA branches separate with increasing P giving increased *aaa* phase space and phonon-phonon

scattering rates (see Figs. S1 and S4 in Ref. 46). The resulting smaller acoustic phonon lifetimes prevail against the increased acoustic velocities giving decreasing κ with P.

Consider how κ and dκ/dP vary as the size of the *a-o* gap is increased [48]. Figure 3 shows the calculated κ at 300K for P=0 and for P=16 GPa of a hypothetical crystal in which BAs IFCs are retained but m_2/m_1 is varied keeping the unit cell mass fixed: $m_1+m_2=m_B+m_{As}$=85.73 amu. This changes the phonon frequencies and the size of the *a-o* gap. For m_2/m_1=1, the *a-o* gap is zero, so both *aao* and *aaa* scattering rates are strong giving much reduced κ compared to the actual BAs compound. Then increasing P increases κ since the reduction in *aao* scattering rates with P has a larger effect than the increase in *aaa* scattering rates. As m_2/m_1 increases, zone boundary LA frequencies decrease while optic frequencies increase. This widens the *a-o* gap causing the *aao* scattering rates to decrease and κ to increase. Also, increasing m_2/m_1 pushes the LA and TA branches together, which decreases the phase space for *aaa* scattering. There is a cross-over in the P=0 and P=16GPa curves at $m_2/m_1\approx5$. For $m_2/m_1<5$, κ increases with P, *i.e.*, dκ/d$P>0$, while for $m_2/m_1>5$ dκ/d$P<0$. This reflects the transition between the region where *aao* scattering dominates ($m_2/m_1<5$) and that where *aaa* scattering dominates ($m_2/m_1>5$). We note that the large mass ratio compounds considered have strong chemical bonds and reasonably small LO-TO splittings. Compounds with weak bonds and/or large LO-TO splittings would require correspondingly larger mass ratios to achieve the freeze-out condition.

The above behavior can be understood qualitatively by examining the three-phonon scattering phase space [49]:

$$\varphi_{jj'j''}^{3-ph} \propto \sum_{\mathbf{qq'}} (\delta(\omega_{\mathbf{q}j} + \omega_{\mathbf{q'}j'} - \omega_{(\mathbf{q+q'-K})j''}) + \frac{1}{2}\delta(\omega_{\mathbf{q}j} - \omega_{\mathbf{q'}j'} - \omega_{(\mathbf{q-q'-K})j''})) \qquad (2)$$

which is constrained by the energy and momentum conservation conditions: $\omega_{\mathbf{q}j} \pm \omega_{\mathbf{q}'j'} = \omega_{\mathbf{q}''j''}$ and $\mathbf{q} \pm \mathbf{q}' = \mathbf{q}'' + \mathbf{K}$ where $\mathbf{K}$ is a reciprocal lattice vector. For small mass ratio, the *aao* processes contribute significantly to φ_{aao}^{3-ph}, and these combined with the *aaa* processes give a large phase space for three-phonon scattering (see Fig 3 inset). With increasing m_2/m_1 the *aao* and, to a lesser extent, the *aaa* phase spaces decrease contributing to the increase in κ seen in Fig. 3. Beyond the *aao* freeze-out condition, only *aaa* scattering occurs giving a phase space that weakly decreases with increasing mass ratio. Table I shows that the *aao* phase space typically decreases with increasing *P* while the *aaa* phase space typically increases with increasing *P* (see Figs. S3 and S4 in Ref. 46).

Why does the LS theory not capture the decrease in κ with *P*? It gives [7, 11]: $\kappa = AV^{1/3}\omega_D^3/(\bar{\gamma}^2 T)$, where A is a constant, ω_D is the acoustic Debye frequency and $\bar{\gamma}$ is a mode-averaged Grüneisen parameter [46]. Upon compression, V decreases, while ω_D increases as phonons are shifted to higher frequencies, and $\bar{\gamma}$ decreases because of the stiffening of the interatomic potential. The decrease in V is more than compensated by the increase from $\omega_D^3/\bar{\gamma}^2$ giving an increased κ. Phonon-phonon scattering rates are affected by anharmonicity and by the scattering phase space. The LS theory represents the anharmonicity through $\bar{\gamma}$. However, it does not capture the details of the three-phonon phase space. This phase space and its changes with *P* can be highly variable across materials. With increasing *P* the energy-momentum conserving surfaces for *aaa* processes become larger. On the other hand, for *aao* processes, the *a-o* gap increases more rapidly than the maximum acoustic frequency, which typically decreases the *aao* phase space. Such changes are not accounted for in LS theory. For small *a-o* gap

materials, they contribute to give $d\kappa/dP>0$, consistent with LS theory. For large *a-o* gap materials, they contribute to give $d\kappa/dP<0$, contrary to LS theory.

Summary—The pressure (P) dependence of the lattice thermal conductivities, κ, of a large number of cubic binary compounds has been studied using an *ab initio* theory of thermal transport. For compounds with similar masses, κ increases with P because anharmonic three-phonon scattering involving two acoustic phonons and one optic phonon (*aao* processes) gets weaker. This increase is consistent with previous measurements and with simple theory. In contrast, for large mass ratio compounds having a large frequency gap between acoustic and optic phonons, *aao* processes do not occur. Then scattering between acoustic phonons limits κ, which decreases with P due to increased scattering phase space. Such behavior is not predicted by the simple theory [11] commonly used to analyze $\kappa(P)$, and it has not been observed previously in crystals far from a pressure-induced phase transition. These results demonstrate the power of *ab initio* methods for elucidating the underlying physics of thermal transport and motivate the growth of new classes of materials with large mass ratios.

Acknowledgements

L. L. acknowledges support from the U. S. Department of Energy, Office of Science, Office of Basic Energy Sciences, Materials Sciences and Engineering Division for work done at ORNL. D.A.B acknowledges support from the National Science Foundation under Grant No. 1402949 and from ONR under grant No. N00014-13-1-0234. NM and JC acknowledge support from Institut Carnot through project SIEVE. T.L.R. acknowledges support from ONR and DARPA. We thank David Cahill and Greg Hohensee for providing the impurity concentrations in their MgO sample. We also thank Saikat Mukhopadhyay and Derek Stewart for kindly providing us with their calculated anharmonic IFCs for BN.

References

[1] P. W. Bridgman, Am. J. Sci. 7, 81 (1924).

[2] D. S. Hughes and F. Sawin, Phys. Rev. 161, 861 (1967).

[3] O. Alm and G. Bäckström, J. Phys. Chem. Solids 35, 421 (1974).

[4] B. Hakansson, P. Andersson, and G. Bäckström, Rev. Sci. Instrum. 59, 2269 (1988).

[5] G. A. Slack and P. Andersson, Phys. Rev. B 26, 1873 (1982).

[6] O. Andersson and A. Inaba, Phys. Chem. Chem. Phys. 7, 1441 (2005).

[7] B. Chen, W. P. Hsieh, D. G. Cahill, D. R. Trinkle, and J. Li, Phys. Rev. B 83, 132301 (2011).

[8] Wen-Pin Hsieh, Ph.D. thesis, Department of Physics, University of Illinois, Urbana-Champaign, 2011.

[9] D. A. Dalton, W.-P. Hsieh, G. T. Hohensee, D. G. Cahill, and A. F. Goncharov, Scientific Reports 3, 2400 (2013).

[10] κ decreasing with P is known to occur for materials approaching a PIPT. In this work, we do not consider such cases.

[11] G. Leibfried and E. Schlömann, Nach. Akad. Wiss. Gottingen, Math. Phyz. Klasse **4**, 71 (1954).

[12] G. A. Slack, in *Solid State Physics*, edited by H. Ehrenreich, F. Seitz, and D. Turnbull (Academic Press, New York, 1979), Vol. 34, pp. 1–71.

[13] J. M. Ziman, *Electrons and Phonons* (Oxford University Press, London, 1960).

[14] M. Omini and A. Sparavigna, Physica B 212, 101 (1995).

[15] M. Omini and A. Sparavigna, Phys. Rev. B 53, 9064 (1996).

[16] D. A. Broido, M. Malorny, G. Birner, N. Mingo, and D. A. Stewart, Appl. Phys. Lett. 91, 231922 (2007).

[17] Wu Li, L. Lindsay, D. A. Broido, D. A. Stewart, and N. Mingo, Phys. Rev. B 86, 174307 (2012).

[18] Z. Tian, J. Garg, K. Esfarjani, T. Shiga, J. Shiomi, and G. Chen, Phys. Rev. B 85, 184303 (2012).

[19] L. Lindsay, D. A. Broido, and T. L. Reinecke, Phys. Rev. Lett. 109, 095901 (2012).

[20] L. Lindsay, D. A. Broido, and T. L. Reinecke, Phys. Rev. B 87, 165201 (2013).

[21] L. Lindsay, D. A. Broido, and T. L. Reinecke, Phys. Rev. B 88, 144306 (2013).

[22] L. Lindsay, D. A. Broido, and T. L. Reinecke, Phys. Rev. Lett. 111, 025901 (2013).

[23] S. Lee, K. Esfarjani, J. Mendoza, M. S. Dresselhaus, and G. Chen, Phys. Rev. B 89, 085206 (2014).

[24] J. Ma, Wu Li, and X. Luo, Appl. Phys. Lett. 105, 082103 (2014).

[25] Wu Li and N. Mingo, Phys. Rev. B 90, 094302 (2014).

[26] J. M. Skelton, S. C. Parker, A. Togo, I. Tanaka, and A. Walsh, Phys. Rev. B 89, 205203 (2014).

[27] X. Tang and J. Dong, Proc. Natl. Acad. Sci. U.S.A. 107, 4539 (2010).

[28] D. A. Broido, L. Lindsay and A. Ward, Phys. Rev. B 86, 115203 (2012).

[29] S. Mukhopadhyay and D. A. Stewart, Phys. Rev. Lett. 113, 025901 (2014)..

[30] S. Baroni, S. Gironcoli, A. D. Corso, and P. Giannozzi, Rev. Mod. Phys. 73, 515 (2001).

[31] http://www.quantum-espresso.org.

[32] P. Giannozzi, S. Baroni, N. Bonini, M. Calandra, R. Car, C. Cavazzoni, D. Ceresoli, G. L. Chiarotti, M. Cococcioni, I. Dabo, A. D. Corso, S. Gironcoli, S. Fabris, G. Fratesi, R.

Gebauer, U. Gerstmann, C. Gougoussis, A. Kokalj, M. Lazzeri, L. Martin-Samos *et al.*, J. Phys.: Condens. Matter 21, 395502 (2009).

[33] P. Hohenberg and W. Kohn, Phys. Rev. 136, B864 (1964).

[34] W. Kohn and L. J. Sham, Phys. Rev. 140, A1133 (1965).

[35] Using Ref. 36, we have estimated fourth-order processes to be much smaller than three-phonon processes for the materials considered here at 300K.

[36] D. J. Ecsedy and P. G. Klemens, Phys. Rev. B 15, 5957 (1977).

[37] The $(d\kappa/dP)/\kappa_0$ values in Table 1 were determined by $(\kappa(P)/\kappa_0-1)/P$. The values of P and $\kappa(P)$ were determined for systems with 3% compressive strain (except GaAs and SiC (1%), and BeSe (5%)). These corresponded to pressures of 19.42 (MgO), 41.55 (BN), 2.53 (GaAs), 7.25 (SiC), 18.46 (BP), 16.09 (BAs), 15.41 (BeSe), 12.09 (BSb) and 6.604 (BeTe) in units of GPa.

[38] R. G. Greene, H. Luo, A. L. Ruoff, S. S. Trail, and F. J. DiSalvo, Phys. Rev. Lett. 73, 2476 (1994).

[39] H. Luo, K. Ghandehari, R. G. Greene, A. L. Ruoff, S. S. Trail, and F. J. DiSalvo, Phys. Rev. B 52, 7058 (1995).

[40] S. Cui, W. Feng, H. Hu, and Z. Feng, Phys. Stat. Sol. (b) 246, 119 (2009).

[41] G. Peckham, Proc. Phys. Soc. 90, 654 (1967).

[42] M. J. L. Sangster, G. Peckham, and D. H. Saunderson, J. of Phys. C: Sol. State Phys. 3, 1026 (1970).

[43] S. Ghose, M. Krisch, A. R. Oganov, A. Beraud, A. Bosak, R. Gulve, R. Seelaboyina, H. Yang, and S. K. Saxena, Phys. Rev. Lett. 96, 035507 (2006).

[44] Impurity concentrations in the MgO sample [9] were determined by G. T. Hohensee and D. G. Cahill, and contain 173.4ppm total impurity concentration consisting of Al, B, Ca, Cr, Fe and Si with primarily Ca (77%) being present. Phonon scattering from impurities was included as substitutions for Mg using the same mass disorder model used for isotopes [21, 45].

[45] S. I. Tamura, Phys. Rev. B **30**, 849 (1984).

[46] See Supplemental Material at http://… for phonon dispersions for BeTe, comparison of *aaa* and *aao* scattering rates, and expression for the averaged Grüneisen parameter.

[47] Wu Li, J. Carrete, N. A. Katcho, and N. Mingo, Comp. Phys. Comm. 185, 1747 (2014).

[48] A. Jain and A. J. H. McGaughey, J. of App. Phys. 116, 073503 (2014).

[49] L. Lindsay and D. A. Broido, J. Phys.: Cond. Mat. 20, 165209 (2008).

Table I Caption

Calculated values for κ_0, the mass ratio, the *a-o* gap (scaled by the largest acoustic frequency), $(d\kappa/dP)/\kappa_0$, comparing *ab initio* values with those from LS theory for several materials at T=300K [37]. The φ_{aaa}^{3-ph} and φ_{aao}^{3-ph} are the three-phonon scattering phase spaces (Eq. 2). The up and down arrows indicate increases or decreases with *P*. Bold red arrows give the type of scattering processes (*aaa* or *aao*) that dominate the behavior of κ with *P*.

	κ_0 ($Wm^{-1}K^{-1}$)	mass ratio	scaled *a-o* gap	$(d\kappa/dP)/\kappa_0$ *ab initio* ($GPa^{-1}\times100$)	$(d\kappa/dP)/\kappa_0$ LS ($GPa^{-1}\times100$)	φ_{aaa}^{3-ph}	φ_{aao}^{3-ph}
MgO	72.45	1.52	0	5.8	3.5	↑	↓
BN	2157	1.30	0	0.9	2.9	↑	↑
GaAs	55.4	1.07	0.09	3.9	19	↓	—
SiC	572.0	2.34	0.19	2.1	3.6	↑	↓
BP	554.1	2.87	0.36	4.1	4.9	↑	↓
BAs	3239	6.93	0.97	-1.9	4.4	↑	N/A
BeSe	621.6	8.76	1.08	-1.6	9.0	↑	N/A
BSb	1087	11.26	1.42	-2.4	5.9	↑	N/A
BeTe	367.6	14.16	1.68	-2.8	15	↑	N/A

Table I

Figure Captions

Figure 1: Calculated phonon dispersions for MgO at P=0 (solid black curves) and P=35GPa, (dashed red curves). Black circles give measured data from Refs. 41 and 42, and red circles give measured data from Ref. 43. Note the upward frequency shifts of phonons with P.

Figure 2: Left panel: Calculated κ (dashed red line) and that including isotopes, impurities and sample boundaries (solid red line), along with measured thermal conductivity (red circles) versus P for MgO [9]. Right panel: κ/κ_0 for BSb (dotted black), BAs (solid orange), BeTe (dashed green) and BeSe (short dashed blue). BeSe has a relatively large contribution to the three-phonon scattering phase space from processes involving one acoustic phonon and two optic phonons. The decrease in this contribution as P increases from zero gives the initial increase in κ seen here in Fig. 2.

Figure 3 Calculated κ versus mass ratio (m_2/m_1) for a hypothetical BAs material for which m_1 (light mass) and m_2 (heavy mass) are varied, but m_1+m_2 stays fixed at $m_1+m_2=m_B+m_{As}$. Solid black and dashed red curves give κ using the BAs IFCs for P=0 and P=16 GPa, respectively. The square symbols on each curve give the calculated κ for the actual BAs mass ratio, m_{As}/m_B=7, which occurs near the freeze-out condition, $\varphi_{aao}^{3-ph}=0$. The inset gives the phase space for *aaa* scattering, φ_{aaa}^{3-ph}, (red curve) and *aao* scattering, φ_{aao}^{3-ph}, (black curve) vs. m_2/m_1 for the hypothetical material for P=0.

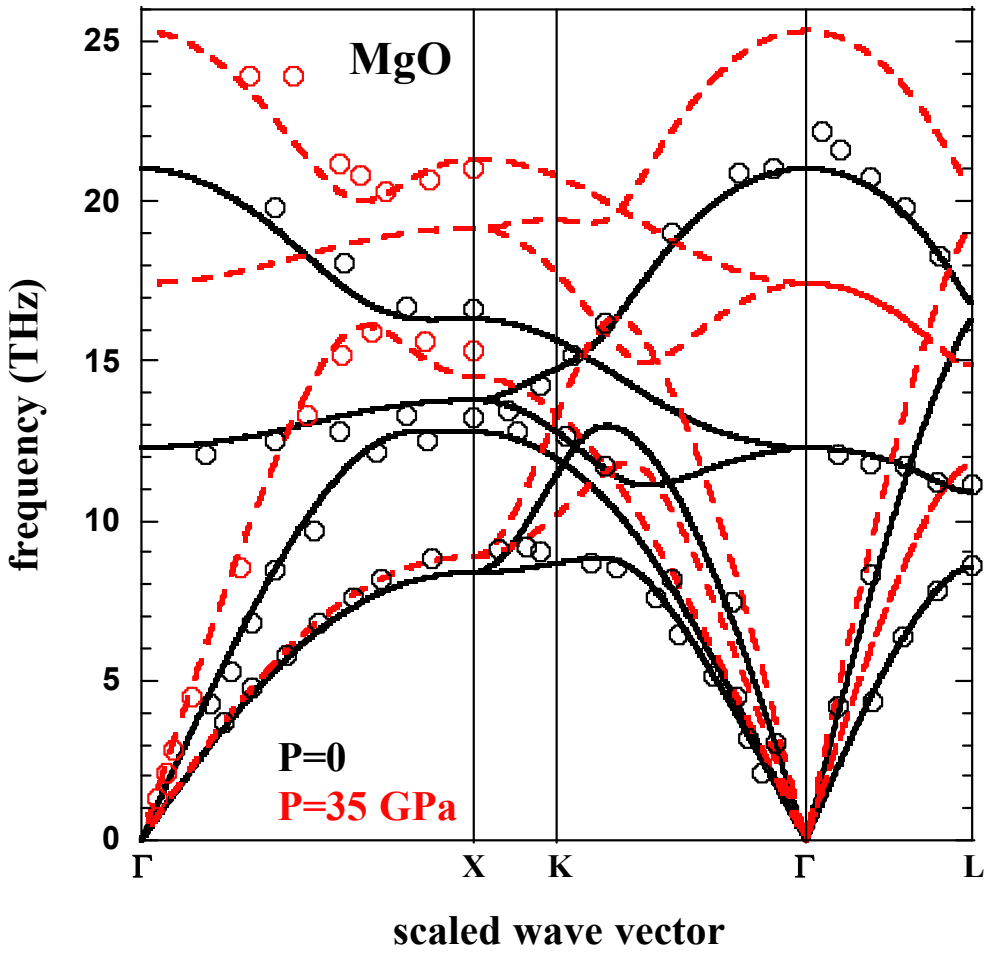
MgO
P=0
P=35 GPa
frequency (THz)
scaled wave vector
0
5
10
15
20
25
Γ
X
K
Γ
L

Figure 1

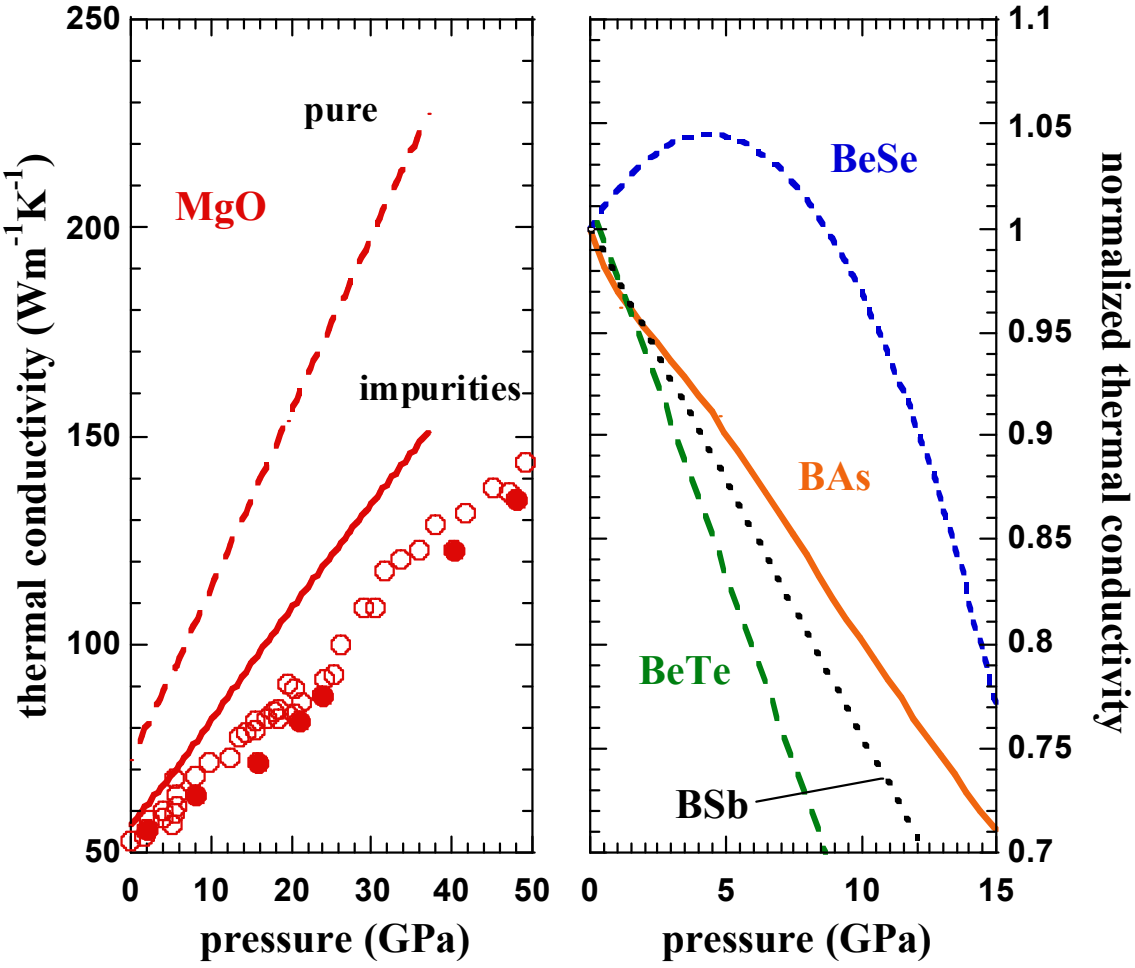
thermal conductivity (Wm^{-1}K^{-1})
250
200
150
100
50
pure
MgO
impurities
0
10
20
30
40
50
pressure (GPa)
1.1
1.05
1
0.95
0.9
0.85
0.8
0.75
0.7
normalized thermal conductivity
BeSe
BAs
BeTe
BSb
0
5
10
15
pressure (GPa)

Figure 2

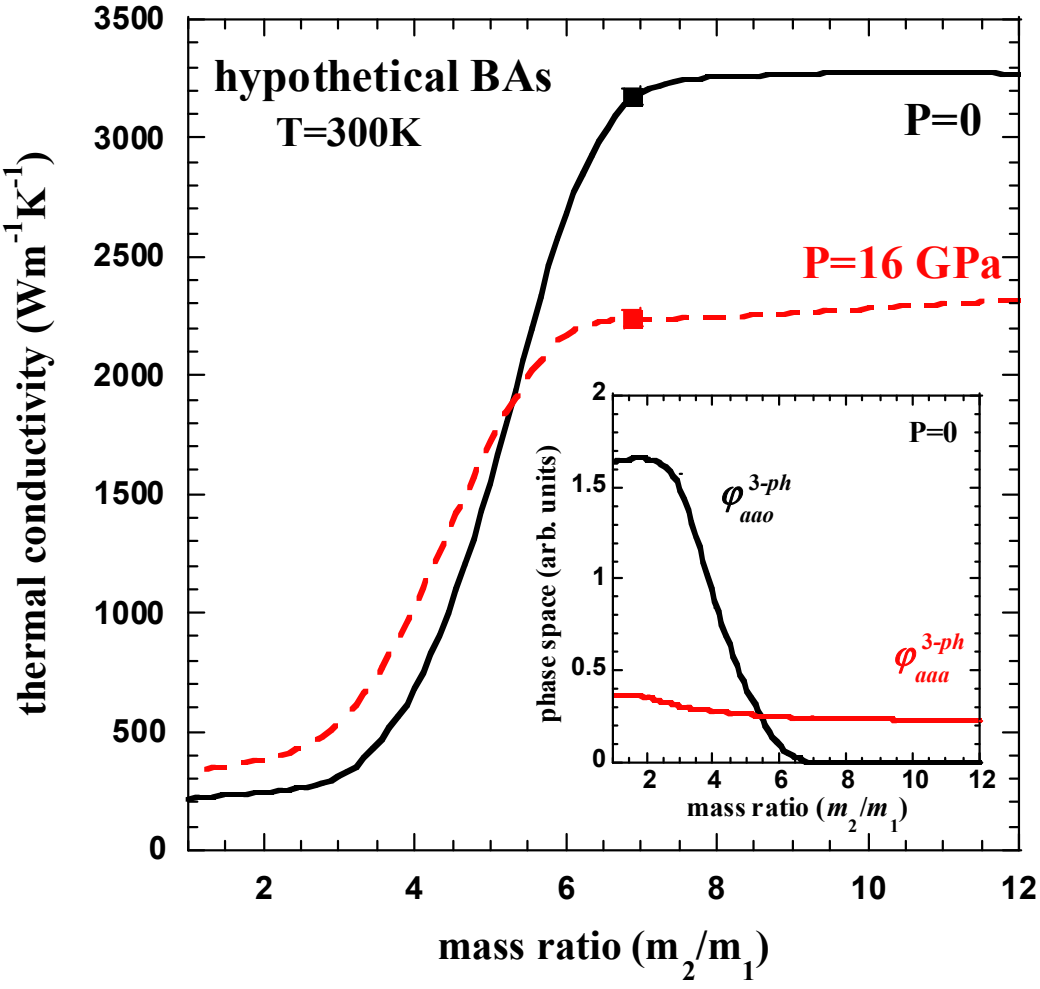
hypothetical BAs
T=300K
P=0
P=16 GPa
thermal conductivity (Wm-1K-1)
mass ratio (m2/m1)
phase space (arb. units)
P=0
φ3-ph aao
φ3-ph aaa
mass ratio (m2/m1)

Figure 3